# 8. REFRACTIVITY IN THE ARCTIC ATMOSPHERE

All electromagnetic radiation (EM) propagation through the atmosphere is affected by the atmosphere. EM energy can be reflected, refracted, scattered, and absorbed by different atmospheric constituents. The extent of these atmospheric effects depends upon both the frequency and power of the EM source and on the state of the atmosphere through which the EM energy must propagate. This chapter summarizes the effects of the environment on E-O, IR, laser, microwave, and radio-wave sensor and communication systems.

In general, environmental effects on communication systems are divided into three categories: attenuation, or loss of energy, of the radiation beam because of beam interaction with absorbing or scattering constituents in the beam path; refraction, or bending of the beam, due to atmospheric density variations along the beam path; and scintillation, or distortion of the beam, due to small scale atmospheric turbulence (Cook and Payne, 1987). Since particulate and density variations are usually greatest in the lower troposphere, it is essential to understand the nature of the atmospheric boundary layer (ABL) in studying electromagnetic propagation. To this end, a discussion of the properties and variations of the ABL will follow the sections on attenuation, refraction, and scintillation.

## 8.1 Attenuation

*Attenuation* is the most important environmental effect on nonlaser visible and IR systems. Small airborne particles (aerosols) and air molecules can remove energy from the radiation beam by scattering the energy out of the beam path and/or absorbing the energy and producing heat. The scattering relationship between aerosols and energy is governed by particle size and energy wavelength. Examples of scattering are the attenuations of visible light by clouds, fog, rain, haze, smoke, and snow.

Atmospheric scattering processes are difficult to quantify and forecast accurately because of the lack of appropriate measurements of particle size distributions and chemical properties. Predictions of attenuation due to scattering for visible wavelengths are operationally derived from atmospheric visibilities, which are related to meteorological conditions as shown in Table 8-1.

**TABLE 8-1. INTERNATIONAL VISIBILITY CODE, VISIBILITY, AND PERCENT ATTENUATION DUE TO SCATTERING FOR A 1 KM PATH**

| Code No. | Weather Condition | Visibility | | 1 km Path Attenuation (%) |
|---|---|---|---|---|
| | | Metric | English | |
| 0 | Dense Fog | <50 m | <50 yd | 100 |
| 1 | Thick Fog | 50 m - 200 m | 50 yd - 219 yd - | >99.99999 - 99.99999 |
| 2 | Moderate Fog | 200 m - 500 m | 219 yd - 547 yd | 99.99999 - 99.9 |
| 3 | Light Fog | 500 m - 1000 m | 547 yd - 1095 yd | 99.9 - 98 |
| 4 | Thin Fog | 1 km - 2 km | 1095 yd - 1.1 nmi | 98 - 86 |
| 5 | Haze | 2 km - 4 km | 1.1 nmi - 2.2 nmi | 86 - 61 |
| 6 | Light Haze | 4 km - 10 km | 2.2 nmi - 5.4 nmi | 61 - 32 |
| 7 | Clear | 10 km - 20 km | 5.4 nmi - 11 nmi | 32 - 18 |
| 8 | Very Clear | 20 km - 50 km | 11 nmi - 27 nmi | 18 - <8 |
| 9 | Exceptionally Clear | >50 km | >27 nmi | <8 |
| — | Pure Air | 277 km | 149 nmi | <1 |

Note: Scattering for moderate to heavy snowfall can be approximated by the figures for light fog.

As the table shows, attenuation at visible wavelengths is practically 100 percent for clouds, fog, and snow. Attenuation at IR wavelengths shows a similar increase from pure air to dense fog, except that clear air is slightly more opaque to IR radiation than to visible, and fog and haze generally are slightly more translucent in the IR.

In addition to scattering by aerosols, IR energy is strongly absorbed by atmospheric water vapor. Water vapor is such an efficient absorber of IR energy that the multiple absorption lines overlap to the point of creating a virtual continuum—an extremely broad band IR absorption feature. Since water vapor is so abundant in the atmosphere, IR systems are confined normally to operating within two minimum absorption windows in the spectrum: 3 to 5 $\mu$m and 8 to 12 $\mu$m.

The attenuation in the 3- to 5-$\mu$m region is generally affected less by water vapor absorption than the 8- to 12-$\mu$m region; however, aerosol scattering and absorption by $CO_2$ molecules is more significant at 3 to 5 $\mu$m. In low latitudes with high water vapor density conditions, the 3- to 5-$\mu$m band is sometimes thought to provide superior transmission because of the heavy absorption of 8- to 12-$\mu$m radiation. Haze affects the 3- to 5-$\mu$m band more than the 8- to 12-$\mu$m band, however, and long haze-free paths through humid atmospheres are rare. The preference in hazy conditions is, therefore, the 8- to 12-$\mu$m band. At high latitudes, the low values of water vapor density again make the 8- to 12-$\mu$m band the preferred choice. Since objects at ambient temperature radiate with their energy peaked in the 8- to 12-$\mu$m band, this window region is a logical choice for target imaging and detection. Hotter targets, such as exhaust plumes, radiate at shorter wavelengths, and when the paths are at high altitudes where the water vapor densities are very low, the 3- to 5-$\mu$m band is preferred.

The attenuation of E-O and IR radiation by atmospheric gases and precipitation as a function of wavelength is depicted in Fig. 8-1. (Attenuation due to dry aerosols, such as pollutants and salt from sea spray, is not shown.) The visible region of the spectrum is transparent in clear air, becomes translucent in the presence of precipitation, and is virtually opaque in dense fog. The same is true for the IR window regions. The far IR and submillimeter wave regions of the spectrum are dominated by water vapor absorption.

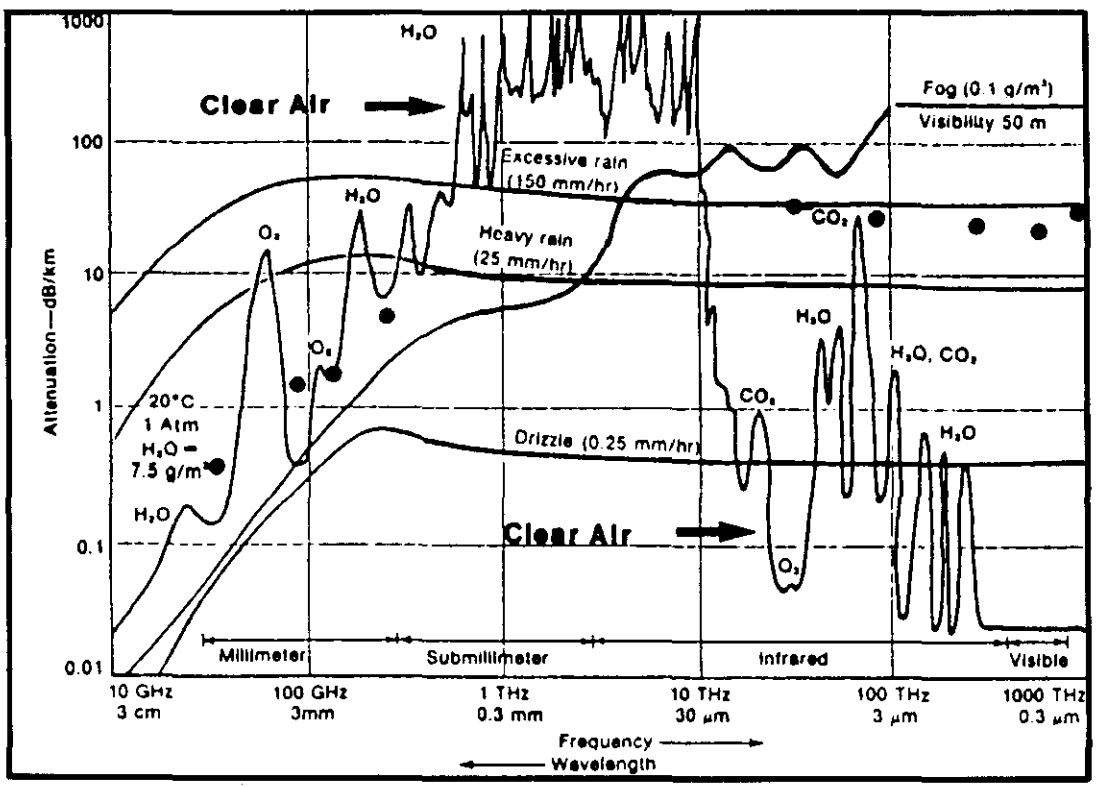


*Figure 8-1. Atmospheric Attenuation at Sea Level.*

Laser beams are also subject to attenuation as previously described. The proper wave band must be chosen to minimize attenuation because other environmental factors also seriously affect beam quality, spot size, and power on target.

Electromagnetic radiation (radar and communications) passing through the atmosphere is depleted by both absorption and scattering, which are caused by gaseous constituents of the atmosphere and by particles carried by the atmosphere. Molecular absorption and scattering have the greatest effect on super high frequency (SHF, 3-30 GHz) and extremely high frequency (EHF, 30-300 GHz) radiation (Fig. 8-2). This absorption involves well-defined frequencies and thus occurs in narrow bands (or lines), primarily attributable to oxygen and water vapor. Since water vapor concentration varies significantly through the atmosphere, absorption by water vapor also varies significantly.

At microwave frequencies (300 MHz-100GHz), scattering and absorption by particles in the atmosphere are dominated by liquid water drops. These droplets scatter wavelengths roughly the same size as the droplets and thus scatter frequencies above about 300 MHz (ultrahigh frequency [UHF] and higher). Other important scattering particulates include smoke, dust, and insects, which primarily affect UHF, although smoke particles also absorb SHF and EHF.

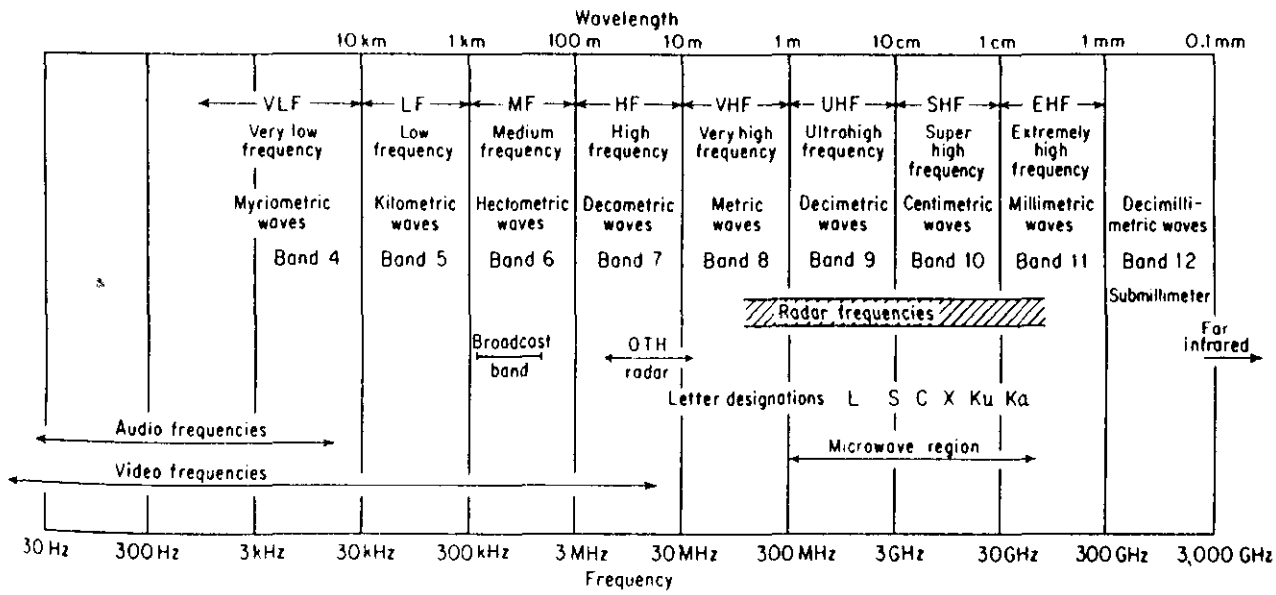


*Figure 8-2. The Electromagnetic Spectrum.*

## 8.2 Refraction

*Refraction* is the bending of light rays due to refractive index (density) changes in the atmosphere. For visible and IR propagation, refraction can cause image distortion, image inversion, and path length changes important for laser ranging. Refractive conditions are characterized by comparison to the refraction expected from a standard atmosphere. Differences from standard conditions are due to temperature and water vapor density fluctuations. Large gradients of these parameters near the ocean surface can seriously affect surface horizontal propagation paths. Propagation over slant paths are usually not seriously affected by refraction.

The index of refraction of a medium, $n$, is defined by Eq. (8.1) where $c$ is the velocity of an EM wave in free space and $v$ is the velocity of the same EM wave in another medium.

$$n = c/v \tag{8.1}$$

For the atmosphere, the refractive index is defined to be the ratio of the velocity of propagation of an EM wave in a free space to that in the air. Since the velocity of an EM wave in free space is always faster than that in any medium, the index of refraction is always greater than one. In the standard atmosphere, a typical near-sea-level value for $n$ is approximately 1.0003 (Bean and Dutton, 1966). For convenience, the refractivity $N$ is defined by Eq. (8.2) such that normal atmospheric values of $N$ units range from 250 to 400.

$$N = (n\text{-}1) * 10^6 \tag{8.2}$$

As stated by Battan (1973), "In dry air the index of refraction has the same value over almost the entire range of the electromagnetic spectrum: it is the same for light and radio waves. However, when water vapor is added to the air, the value of $N$ for the mixture becomes frequency dependent. It is well known that the water vapor molecule is polar in nature and that the dipole moment of the molecule has a different response to different frequencies of radio waves. With the extremely high frequencies of visible light, the water molecules are electronically polarized. With the lower frequencies of radar waves, the water molecules not only acquire electronic polarization, but also reorient themselves rapidly enough to follow the electric-field changes. As a result, the index of refraction of water vapor is greater for radio than for optical frequencies."

Temperature, water vapor, and pressure are the major variables of the atmosphere that determine its refractivity. Bean and Dutton (1966) expressed refractivity in terms of temperature $T$ in Kelvin, with pressure $P$, and water vapor pressure $e$, in millibars as follows in Eq. (8.3):

$$N = 77.6\ P/T - 5.6\ e/T + 3.75 * 10^5\ e/T^2 \tag{8.3}$$

In an atmosphere of constant $N$ units, no bending of an EM wave could occur regardless of the value of $N$. Refraction is dependent upon the gradients of $N$.

Since gradients of pressure, temperature, and humidity occur throughout the atmosphere, it follows that gradients of $N$ must also exist. Battan (1973) showed that when the gradient of $N$ (i.e., $dN/dZ$) is equal to $-157$ km$^{-1}$, a propagating EM wave will bend with a curvature exactly equal to that of the Earth. Bending would cause a horizontally propagating EM wave to remain constantly parallel to the Earth's surface, always at the same height. Any value of $dN/dZ$ less than $-157$ km$^{-1}$ would cause an EM wave to bend with greater curvature than the Earth's surface; therefore, $-157$ km$^{-1}$ is the threshold for "trapping" of an EM wave.

Trapping, or ducting, occurs when the microwave energy is trapped in layers and propagates to greater ranges than normal because of the lack of vertical spreading of the rays. Ducting regions can be elevated or surface based. Radar propagation and coverage are affected by the refractive nature of the atmosphere. Nonstandard refractive conditions lead to anomalous propagation and can cause microwaves to be refracted less than normal (subrefraction), refracted more than normal (superrefraction), or trapped in wave-guide modes (ducted) as in Fig. 8-3.

Over the oceans, a persistent surface ducting mechanism is the rapid, near-surface decrease in moisture due to evaporation, which creates evaporation ducts. The relation for the vertical gradient of refractivity as a function of $T$, $P$, and specific humidity ($q$) is given by Eq. (8.4).

$$dN/dZ = 0.3\ dP/dZ + 7.2\ dq/dZ - 1.3\ dT/dZ \tag{8.4}$$

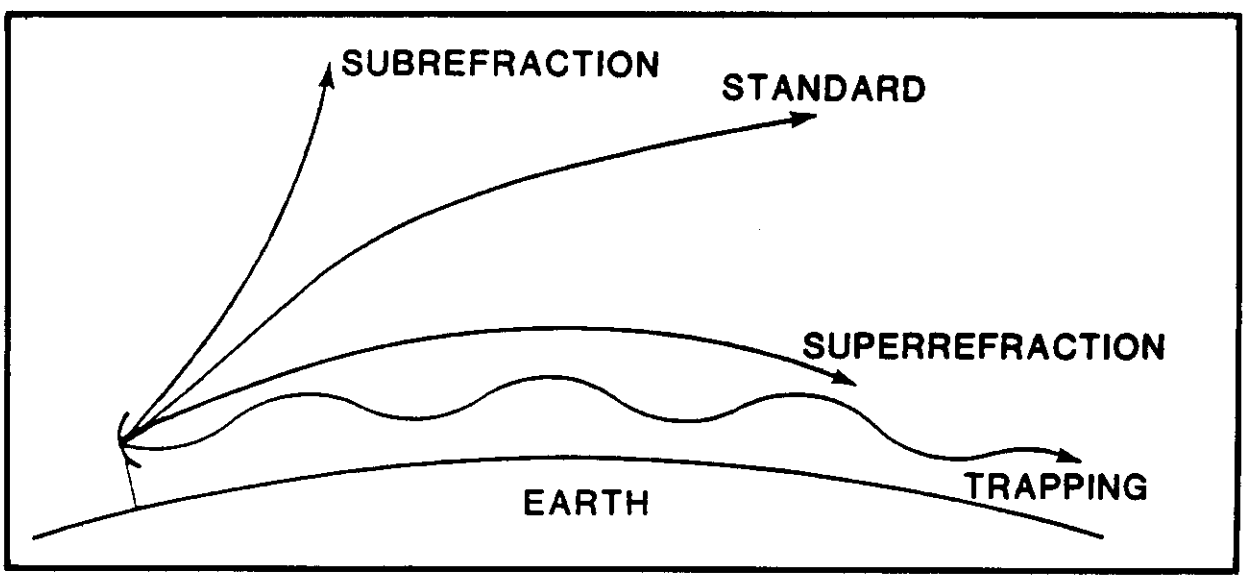


*Figure 8-3. Four Basic Categories of Refraction.*

It is sometimes convenient to think of the Earth's surface as flat and to represent the EM wave refraction in this frame of reference. This conversion can be done simply by subtracting the Earth's curvature from the EM wave and from the Earth. A modified refractivity $M$ has been developed to take into account the Earth's curvature and to allow for easy identification of ducting. Eq. (8.5) shows the relationship of $M$ to $N$ (Battan, 1973).

$$M = N + 157Z, \; Z \text{ in km} \tag{8.5}$$

## 8.3 The Integrated Refractive Effects Prediction System

The Integrated Refractive Effects Prediction System is a shipboard environmental data processing and display system that is used to predict the effects of refraction on EM signals for naval surveillance, communications, electronic warfare, and weapons guidance systems. Environmental data usually obtained from radiosondes are processed on a desk-top computer, the Hewlett-Packard 9845, to derive a comprehensive assessment of refractive effects in the lower atmosphere. Knowledge of the refractive environment can be used to maximize tactical advantage. The most recent IREPS, version 2.2, is an integral part of the Tactical Environmental Support System (TESS), now being introduced into the fleet.

IREPS uses $M$ gradients to classify refractive conditions. Table 8-2 shows IREPS classifications of refractive conditions and the relationship of $N$ units to $M$ units.

**TABLE 8-2. IREPS CLASSIFICATION OF REFRACTION CONDITIONS**

| IREPS Classification | dN/dZ $km^{-1}$ | dM/dZ $km^{-1}$ | Range |
|---|---|---|---|
| Subrefraction | $>0$ | $>157$ | Reduced |
| Normal | 0 to $-79$ | 79 to 157 | Normal |
| Superrefraction | $-79$ to $-157$ | 0 to 79 | Increased |
| Trapping | $<-157$ | $<0$ | Greatly Increased |

The performance of the IREPS model is directly related to the quality and timeliness of atmospheric information entered into the program. Accurate and timely data must be used if the resulting displays are to indicate the true refractive structure of the atmosphere. Knowledge of the immediate environment and its dynamic evolution are necessary for a proper interpretation of IREPS results.

By comparing the IREPS version 2.2, computed atmospheric refractivity conditions for a high resolution and degraded resolution sounding, Dotson (1987) showed the importance of high resolution data. The high resolution data were better able to define the smaller scale refractive structure of the atmosphere and, therefore, allowed IREPS to realistically portray the ambient ducting conditions. By observing the variability in ducting conditions for 120 soundings taken at irregular time intervals over a 47-day period, Dotson found that refractive conditions are in constant dynamic evolution on diurnal as well as synoptic time scales. This discovery implies that timely data must be used to achieve accurate refractivity condition predictions. Contrary to previous arguments that in over 85 percent of the time the horizontal homogeneity was not a factor in refractive considerations, Dotson found that horizontal inhomogeneity does indeed cause significant variability in radar lobe coverage at least 50 percent of the time when near areas of weak sea surface temperature gradients.

Ducting is of primary concern to Navy operations and is caused by trapping layers. A trapping layer is defined as the area where $M$ decreases with height ($dM/dZ < 0$). In this region the ray is bent downward relative to the Earth's surface. A duct is defined as the region in which the energy is confined. A surface-based duct occurs when an EM wave is refracted downward at a curvature greater than the Earth's curvature and is then subsequently reflected up from the Earth's surface. It is the continuous refraction down and the reflection up that forms the duct and makes ducting a concern to the Navy by allowing detection by surface radars far beyond the normal horizon. The type of duct depends on the height, strength, and extent of the trapping layer.

The top of the duct is defined as the height where $M$ reaches a minimum value. It also corresponds with the top of the trapping layer. In practice, thickness of the duct may be found by dropping a vertical line from the top of the duct down toward the surface until it intersects the $M$ profile. Duct strength is defined as the maximum range of $M$ values within the limits of the duct. The optimum coupling height (OCH) is the height where the $dM/dZ$ profile changes from a positive to a negative value.

Three types of ducts commonly exist: (1) the surface-based duct, (2) the elevated duct, and (3) the evaporative duct. Profile (a) of Fig. 8-4 depicts an *elevated* duct that is the type often found when an inversion layer is present. Large temperature and humidity gradients are usually present within the inversion. The boundary layer is cool and moist relative to the overlying air, and over the ocean it is often referred to as the MARINE layer. These jumps in the vertical structure of the temperature and humidity are associated with warming and drying due to subsidence above the inversion and turbulent mixing in the boundary layer. In the Arctic this type of ducting, which causes strong subsidence, is most likely when the Greenland High is well established.

Profile (b) of Fig. 8-4 is an example of a *surface-based* duct. These ducts are formed by relatively warm, dry air being advected over a cool body of water, or by strong subsidence modifying the elevated duct.

Figure 8-4(c) shows an *evaporative* duct. The evaporative duct can be created by two different mechanisms. First, an evaporative duct may be created by the very rapid decrease of moisture immediately above the ocean surface. The air adjacent to the ocean is saturated with water vapor, and the relative humidity is 100 percent. This high relative humidity decreases rapidly in the first few meters to an ambient value that depends on varying

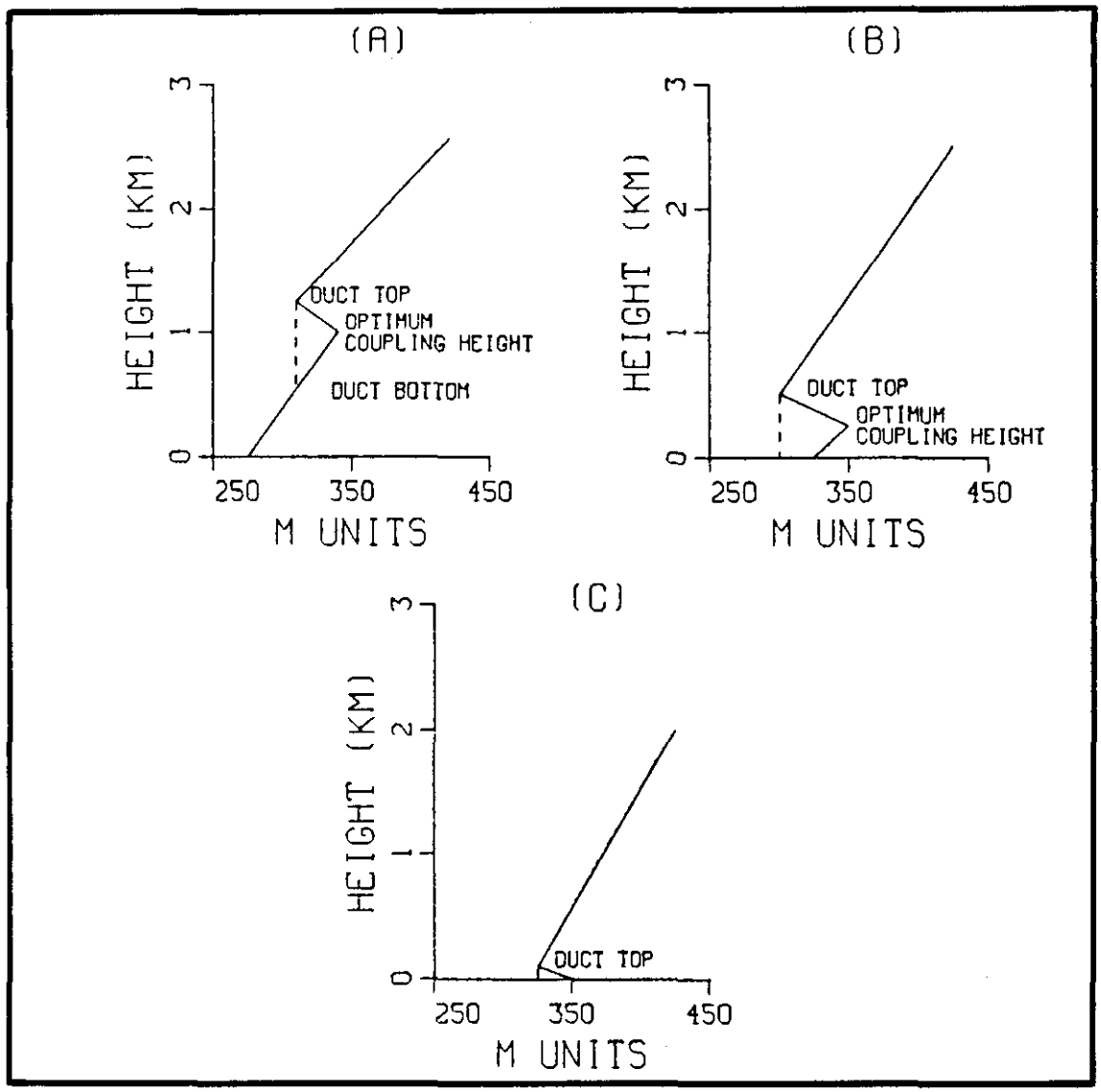


*Figure 8-4. Ducting Occurrences for Typical M Profiles.*

meteorological conditions. This initial rapid decrease in humidity will cause *M* to decrease with height to a minimum and then *M* will increase with height. The second way in which an evaporative duct can be formed is independent of the decrease in humidity. This evaporative duct is caused by strong cooling at the surface. The cooling can cause a sufficient positive temperature gradient between the air near the surface and the air just above to create a duct. Radiation fog is often associated with this condition because the overlying air is cooled sufficiently by radiational transfer for the relative humidity to increase to the point of condensation. Evaporative ducts almost always occur over the oceans, but it is the strength and upper boundary that are critical in determining the importance of this duct to tactical operations. The evaporative duct, although present, is generally shallow in the Arctic.

Two other important refractive effects are subrefraction and superrefraction. *Subrefraction* is defined as $N$ increasing with height as shown in Table 8-2. In this situation the rays actually bend away from the Earth's surface. The radar range in this situation is reduced. *Superrefraction* is defined in Table 8-2 as $N$ gradients having values between $-79$ to $-157$ per km. The EM wave is bent toward the Earth's surface, but not strongly enough to form a trapping layer. With superrefraction the radar range is increased somewhat. The refractive conditions vary from one location to another. In Section 8.6, the assumption made by IREPS that horizontal homogeneity is valid 85 percent of the time is shown NOT to be valid in the Arctic.

## 8.4 Description of Some IREPS Output Products

Figure 8-5 is a representation of one type of IREPS product. The environmental data list is used primarily for checking the numerical values of the input data. The IREPS-computed output values of dewpoint depression, *dN/dZ* values, *M* units, and a single word description of the refractive conditions give an overall assessment of the atmospheric refractive conditions from each input level to the next.

IREPS REV 2.2

**** ENVIRONMENTAL DATA LIST ****

LOCATION: 31 56N 118 36W
DATE/TIME: 17 JUN 0045Z

WIND SPEED 12.0 KNOTS

EVAPORATION DUCT PARAMETERS:
SEA TEMPERATURE 18.2 DEGREES C
AIR TEMPERATURE 15.1 DEGREES C
RELATIVE HUMIDITY 89 PERCENT
EVAPORATION DUCT HEIGHT 28.0 FEET

SURFACE PRESSURE = 1008.0 mB
RADIOSONDE LAUNCH HEIGHT = 60.0 FEET

| LEVEL | PRESS (mB) | TEMP (C) | RH (%) | DEW PT DEP(C) | FEET | N UNITS | N/Kft | M UNITS | CONDITION |
|---|---|---|---|---|---|---|---|---|---|
| 1 | 1,008.0 | 15.1 | 39.0 | 1.8 | 60.0 | 340.0 | -28.2 | 342.9 | SUPER |
| 2 | 1,000.0 | 14.2 | 87.0 | 2.1 | 281.6 | 333.8 | 15.6 | 347.2 | SUB |
| 3 | 993.0 | 13.9 | 95.0 | 0.8 | 476.6 | 336.8 | -10.9 | 359.6 | NORMAL |
| 4 | 982.0 | 13.3 | 97.0 | 0.5 | 785.3 | 333.4 | -176.4 | 371.0 | TRAP |
| 5 | 972.0 | 20.4 | 25.0 | 20.8 | 1,071.8 | 292.9 | 27.2 | 334.2 | SUB |
| 6 | 962.0 | 21.5 | 34.0 | 16.6 | 1,364.9 | 290.9 | -28.9 | 356.2 | SUPER |
| 7 | 949.0 | 21.5 | 27.0 | 19.9 | 1,751.3 | 279.7 | -9.4 | 363.5 | NORMAL |
| 8 | 862.0 | 20.6 | 25.0 | 20.8 | 4,477.3 | 254.0 | -9.5 | 468.2 | NORMAL |
| 9 | 850.0 | 19.7 | 25.0 | 20.7 | 4,873.5 | 250.2 | -7.6 | 483.4 | NORMAL |
| 10 | 807.0 | 20.0 | 25.0 | 20.7 | 6,339.1 | 239.0 | -6.0 | 542.3 | NORMAL |
| 11 | 726.0 | 14.5 | 34.0 | 15.8 | 9,299.4 | 221.2 | -8.9 | 666.1 | NORMAL |
| 12 | 700.0 | 11.8 | 34.0 | 15.5 | 10,305.6 | 212.2 | ------ | 705.3 | ------ |

SURFACE REFRACTIVITY: 341 --SET SPS-48 TO 344

*Figure 8-5. IREPS Environmental Data List.*

The propagation conditions summary, reproduced in Fig. 8-6, is a system independent visual display and plain-language narrative assessment of expected refractive conditions. Vertical profiles of refractivity *N*, as well as modified refractivity *M*, are accompanied by a diagram showing the presence and vertical extent of any existing ducts. Evaporation duct height and surface wind speed information is given along with brief statements concerning anticipated performance of surface to surface, surface to air and air to air EM systems.

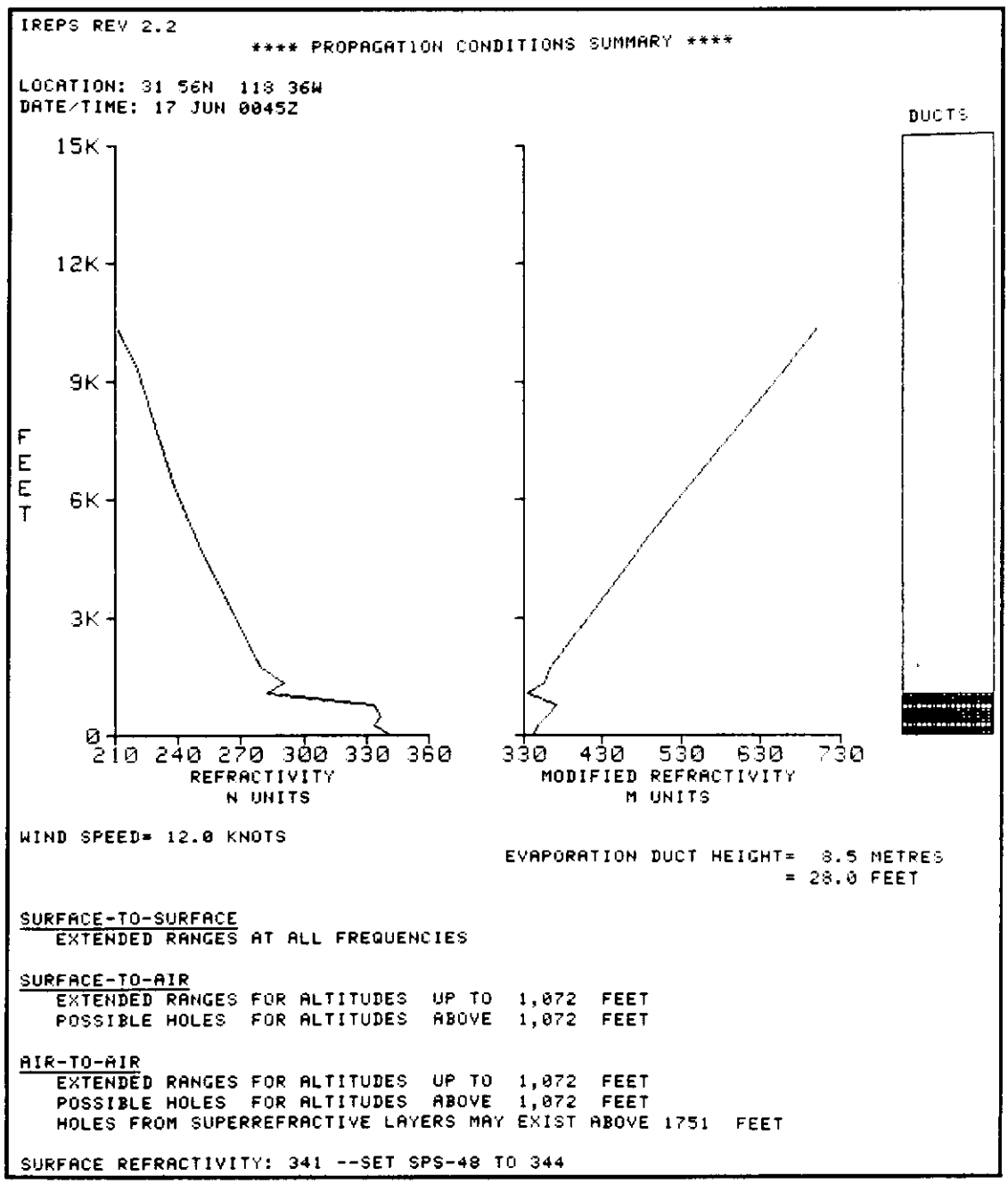


*Figure 8-6. IREPS Propagation Conditions Summary.*

Propagating radar waves experience constructive and destructive interference as direct path rays coincide with rays reflected from the sea surface. The resultant amplitude of the radar wave is a function of the phase differences among the intersecting waves. As a result, radar lobes (constructive interference) are created with shadow zones (destructive interference) appearing in between. Knowledge of where these lobes and shadow zones occur can become an immediate tactical advantage in both offensive and defensive operations. IREPS version 2.2 produces radar coverage diagrams that display the positions of the lobes and the shadow zones for any specified radar system and target at any desired probability of detection (POD).

Since these lobes and shadow zones are created by reflections from the sea surface, their extent is determined by the roughness of the sea surface. Surface roughness is dependent on the sea state and wind speed, with higher wind speeds and rougher seas leading to relatively reduced coverage; low wind speeds and calm seas lead to relatively increased coverage. Wind speed changes are important indicators of changing radar conditions *not dependent* on refractivity.

Figure 8-7 is an example of the IREPS radar coverage display product that also can be very useful in determining an EM system's maximum range capability. It depicts a specified EM system's area of coverage on a curved Earth, range-versus-height plot. Varying PODs are indicated by variations in the shading of the lobes. A numeric listing of some of the parameters used to generate the display, along with the location and time/date information of the profile, are included at the top and bottom of this product.

## 8.5 Atmospheric Boundary Layer

Propagating EM waves, unless in a completely homogeneous medium, will experience some degree of bending due to changes in the index of refraction. The Earth's atmosphere is normally a very inhomogeneous fluid. Certain regions, such as the ABL, characteristically have large mean gradients in temperature and/or humidity. Rapid vertical changes in both temperature and humidity create layers that significantly refract propagating EM signals. This phenomenon is readily apparent, for example, in the evaporation duct at the base of the Marine Atmospheric Boundary Layer (MABL) and in the elevated trapping layer associated with the inversion layer at the top of the ABL.

The ABL is defined by Stewart (1979) as the portion of the lower atmosphere that has turbulent flow and is in direct contact with the Earth's surface. The ABL extends from the surface to a height of a few meters in conditions of strongly stable stratification and to thousands of meters in highly convective conditions. On the average, the ABL extends through the lowest 3,300 ft ($\approx$ 1 km) of the atmosphere and contains 10 percent of the mass of the atmosphere. The boundary layer is very important to the dynamics and thermodynamics of the atmosphere because it is in this layer that all momentum, water vapor, and thermal energy exchanges between the atmosphere and the Earth's surface takes place.

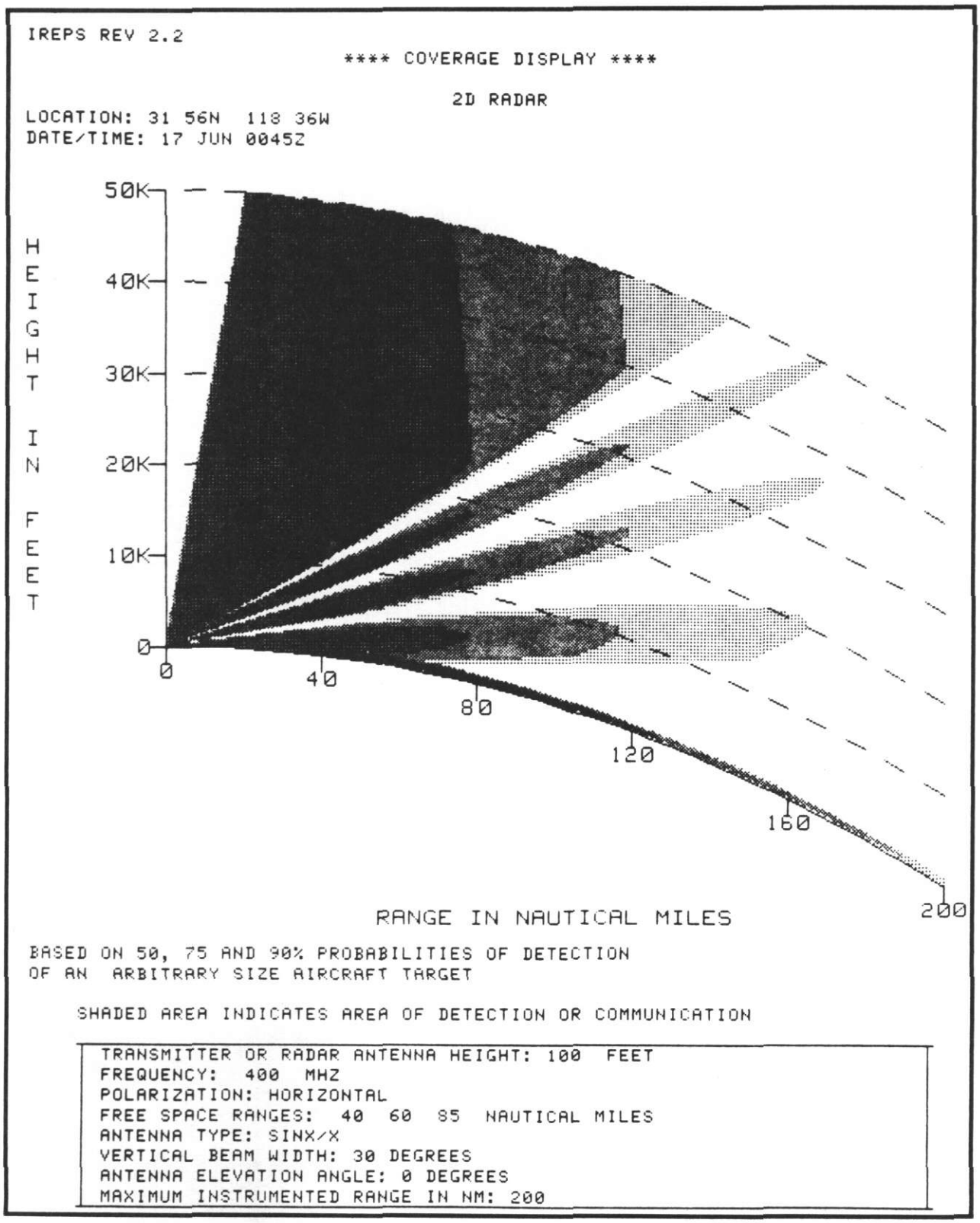


*Figure 8-7. IREPS Radar Coverage Diagram.*

Physical continuity between the atmosphere and the Earth dictates that wind velocity be zero at the immediate surface over land and equal to the surface drift current over water. Above the surface, velocity increases with height in an approximately logarithmic fashion to the top of the layer. Thus, strong vertical wind shear is common in this layer. It, along with convection, produces turbulence that facilitates the transport of moisture and momentum within the layer. The relatively homogeneous mixed layer directly above the turbulent surface layer constitutes the majority of the unstable ABL. Turbulence tends to continuously erode local gradients and, thus, conditions are well mixed up to the inversion layer. The final 165 to 325 ft ($\approx$ 50–100 m) of the convective ABL is usually an inversion layer where the kinetic energy available for mixing is damped by strong stable vertical temperature gradients. The gradients have a "capping" effect on the convection below and effectively suppress exchange of physical properties with the free atmosphere above.

If the ABL is cooled from below it will be stable. Turbulence is suppressed by the resulting density structure, and generally little mixing will occur except in the surface layer. All exchanges between the atmosphere and the Earth's surface are thus greatly reduced.

In the marine atmospheric boundary layer the oceans and the atmosphere exchange energy directly in the form of turbulent heat, moisture, and momentum fluxes. Gases and solids are also in continuous exchange between each fluid. Wave activity can toss small water droplets directly into the lower atmosphere where they become suspended and eventually evaporate. Normally, evaporation from the sea surface creates a shallow layer of rapidly decreasing relative humidity, from 100 percent at the sea surface to a lower value (80–90 percent) directly above the sea surface. This low level feature produces an extended radar propagation phenomenon known as the evaporation duct because of its formation mechanism. The evaporation duct extends only tens of meters above the ocean's surface, but it is of great importance to the mariner because it occurs in varying degrees throughout all oceanic areas and results in over-the-horizon radar propagation.

The ABL over land shows much more variation than the MABL. Seasonal and diurnal changes are both more pronounced. Larger variations in the vertical temperature structure occur over land than over the ocean, but usually less vertical humidity variation occurs. Radiative heating and cooling can cause large diurnal fluctuations in the height of the ABL from near surface values at night to over 6,500 ft ($\approx$ 2000 m) during the day.

## 8.6 Arctic Refractive Conditions

Willis (1987) examined the spatial and temporal variability of the refractive structure of the lower atmosphere in the vicinity of the Fram Strait MIZ. The data used in this study were collected by four ships during MIZEX of 1984. The ships operated in the pack ice, at the MIZ, and in the water adjacent to the ice edge.

The results of a spatial study showed that the refractive structure leading to elevated ducting was different over the pack ice and the MIZ from over the open water adjacent to the ice edge. The ducts were generally lower, weaker, and thinner over the pack ice, with the averages of height, strength, and thickness dramatically increasing over the water,

away from the ice edge. Scatter diagrams showed that the duct height, strength, and thickness exhibited a linearly increasing relationship with respect to distance from the ice. The average height, strength, and thickness values increased slightly from the pack ice to the MIZ and then dramatically increased from the MIZ to 115 n mi ($\approx$ 210 km) from the ice edge. This linearly increasing relationship from the pack ice to the open water was strongest with the height data. These differences in the refractive structure over this relatively narrow region are tactically important. An EM wave transmitted from a source located over the ice would be affected differently from an EM wave transmitted from a source over the water. Multiple ducts were seen only at the ice edge and may have reflected the multiple inversions that were seen on sodar traces.

Willis (1987) also made a temporal study by selecting six regimes to assess the effect of the difference in synoptic flow on the refractive structure. In four of six regimes a cyclone passed over the area. When the low passed directly over all four of the ships no ducts were recorded. The greatest number of ducts was associated with the two regimes in which high pressure dominated the period. This situation was the only one in which persistence of the ducts was seen. On two separate occasions two ships reported ducts that persisted for 24 hours. At both of these times, however, only two of the four ships reported ducts; so once again considerable spatial inhomogeneity existed. The longest case on record in which a duct persisted was 36 hours.

Shaw et al. (1989) has presented some results of refractive studies carried out during MIZEX of 1984 and 1987. Several conclusions were drawn from that work derived from numerous summer/winter radiosonde records.

1. Substantial difficulty may occur in obtaining accurate refractivity profiles from rawinsondes in the Arctic if the sensors pass through subfreezing stratus clouds. Many launches from MIZEX of 1984 produced profiles that may indicate erroneous saturation due to frost formation on the humidity sensor.
2. Irrespective of the frost formation problem, trapping layers in the MIZ of the Arctic are in general quite weak and occur within 30 n mi ($\approx$ 56 km) of the ice edge. Furthermore, they occur typically 1,000 to 2,600 ft (300–800 m) above the surface, making them unlikely to affect surface-based microwave devices. There is, however, a decidedly upward slope from ice (shallow boundary layer) to water (deeper boundary layer) of the trapping layer, and this feature may indeed affect surface systems that are well into the ice. Trapping layers are also sporadic in extent. During the 1984 experiment the four ships making measurements never observed a trapping layer at the same time. The majority of the time (61 percent) only one ship observed a trapping layer, and during the remaining time two ships observed a trapping layer concurrently.
3. Horizontal homogeneity is observed less than 13 percent of the time in the Arctic at levels above 65,000 ft ($\approx$ 20 km).

From the Willis and Shaw studies, clearly, anomalous refraction will be of less consequence in the MIZ than in warmer regions of the globe. Equally clear, however, when anomalous refraction is important it will be due largely to horizontal variability of the refractivity field.